

Published in final edited form as:

Nat Cell Biol. 2008 February 01; 10(2): 170–7. doi:10.1038/ncb1678.

Wingless Secretion requires endosome-to-Golgi retrieval of Wntless/Evi/Sprinter by the retromer complex

Xavier Franch-Marro^{#1}, Franz Wendler^{#1,+}, Sonia Guidato¹, Janice Griffith², Alberto Baena-Lopez¹, Nobue Itasaki¹, Madelon M. Maurice², Jean-Paul Vincent^{1,+}

¹MRC National Institute for Medical Research, Mill Hill, London NW7 1AA, UK ²Department of Cell Biology, University Medical Center Utrecht (UMCU), Heidelberglaan 100, 3584CX Utrecht, The Netherlands

These authors contributed equally to this work.

Abstract

The glycolipoproteins of the Wnts family raise interesting trafficking issues, especially with respect to spreading within tissues. Recently, the retromer complex has been suggested to participate in packaging Wnts into long-range transport vehicles^{1,2}. Our analysis of a *Drosophila* mutant in *Vps35* show that, instead, the retromer complex is required for efficient progression of Wingless (a *Drosophila* Wnt) through the secretory pathway. Indeed expression of *senseless*, a short-range target gene³, is lost in *Vps35*-deficient imaginal discs. By contrast, *Vps35* is not required for Hedgehog secretion, suggesting specificity. Overexpression of Wntless, a transmembrane protein known to be specifically required for Wingless secretion^{4–6} overcomes the secretion block of *Vps35* mutant cells. Furthermore biochemical evidence confirms that Wntless engages with the retromer complex. We propose that Wntless accompanies Wingless to the plasma membrane where the two proteins dissociate. Following dissociation from Wingless, Wntless is internalised and returns to the Golgi apparatus in a retromer-dependent manner. Without the retromer-dependent recycling route, Wingless secretion is impaired and, as electron microscopy suggests, Wntless is diverted to a degradative compartment.

Wnt proteins are secreted glycolipoproteins that act as signalling molecules in a variety of developmental processes (<http://www.stanford.edu/~rnusse/wntwindow.html>). Some Wnts, such as *Drosophila* Wingless are known to spread within tissues over many cell diameters^{7,8}. For example, in wing imaginal discs, Wingless forms a concentration gradient that is essential for the growth and patterning of this tissue. The cell biological parameters that control the spreading of Wingless (and of other morphogens) have been the subject of intense investigation^{9,10}. Interest in this issue has been further heightened by the discovery that Wnts undergo up to two lipid modifications^{11,12}. Indeed, the presence of lipid moieties is bound to affect trafficking and spreading along epithelia. One current hypothesis is that Wingless is transported by lipoprotein particles¹³, which would shield the lipid

*Corresponding authors.

moieties thus reducing membrane anchoring of Wingless. This would prevent retention at the site of production and allow transport/diffusion within the extracellular space.

Long-range action of EGL-20, a *C. elegans* Wnt, is preferentially impaired in retromer-deficient worms^{1, 2} while short-range action appears to be unaffected¹. This led to the suggestion that a retromer-dependent process might be required for Wnt-producing cells to package Wnts into lipoprotein particles^{1, 14, 15} prior to dispatching to distant receiving cells. Irrespective of the validity of this suggestion, the phenotype of retromer-deficient worms suggests a novel function for the retromer complex, which has so far been known to direct the retrieval of cargo receptors from endosomes back to the Golgi. One classic example is the cation independent mannose-6-phosphate receptor (CI-MP), which shuttles between endosomes and the Golgi to ensure the continuous delivery of its cargo, lysosomal hydrolases, to the lysosomal compartments^{16, 17}. To precisely assess how the retromer complex modulates the range of Wnts, we turned to *Drosophila*, where the range of morphogens is extensively studied. We generated a null mutation in the *Drosophila Vps35* locus (see materials and methods), a key component of the retromer complex and analysed how loss of *Vps35* affects the spread of Wingless and its range of action in wing imaginal discs.

Homozygous *Vps35* mutants develop melanotic tumors during late larval stages (Fig. 1a, b) and die as prepupa. Survival to such late stages is likely due to the presence of maternally deposited *Vps35*. Indeed, removal of maternal *Vps35* in germ line clones leads to lethality at the end of embryogenesis. The most obvious phenotype at this stage is a failure to assemble cuticle (data not shown), thus precluding an assessment of potential patterning defects in cuticle preparations. Staining with anti-Wingless shows that, by comparison to control wild type embryos, embryos lacking maternal and zygotic *Vps35* accumulate excess Wingless protein (Fig. 1c, d). This indicates that Wingless trafficking might be affected in the absence of *Vps35* activity. As an additional functional assay, we generated clones of homozygous *Vps35* mutant cells during larval stages and examined the phenotype of surviving adults. These often displayed notched wings (Fig. 1e, f), another indication that Wingless function might be affected. We were therefore spurred to proceed with a detailed analysis of the *Vps35* phenotype in developing wing imaginal discs.

To facilitate the phenotypic analysis, we targeted the mutant clones solely in the posterior compartment by inducing FRT-mediated mitotic recombination with *hedgehog-Gal4* and *UAS-Flp*. A cell lethal mutation on the homologous *Vps35*⁺ chromosome ensured the elimination of the wild type twin clones (see materials and methods). In this experimental setup, most of the posterior compartment becomes deficient in *Vps35* (although in some discs a few wild type, GFP-positive cells remain) while the anterior compartment can be used as an internal control. These discs were stained with anti-Wingless using a conventional protocol that reveals both intracellular and extracellular Wingless. As in embryos, in the absence of *Vps35*, imaginal disc cells that normally express *wingless* seem to accumulate excess Wingless protein. (Fig. 1g, h; mutant territory marked with -/-). Discs of the same genotype were also processed for *in situ* hybridization with a *wingless* probe and no increase in transcription was detected in the *Vps35* mutant compartment (Supplementary Fig. 1). Therefore, Wingless accumulation in *Vps35*-deficient cells is not

due to increased transcription. Despite the increased level of Wingless protein in producing cells, non-expressing, signal receiving cells have reduced staining. Note the relative lack of punctate staining in the *Vps35* mutant territory (quantified in the fluorescent profile; inset in Fig. 1h). This observation suggests that Wingless secretion could be impaired in the absence of *Vps35* activity.

Discs with a *Vps35*-deficient posterior compartment were then subjected to a staining protocol that specifically reveals extracellular Wingless⁷. A significant reduction of extracellular Wingless was observed in the mutant compartment (Fig. 1k, l). Residual staining suggests either that *Vps35* is not absolutely required for Wingless secretion or that *Vps35* activity is not completely eliminated in this experiment because of perduring maternal product. Nevertheless, impairment in retromer function clearly leads to a reduction of extracellular Wingless as well as an accumulation of intracellular Wingless in expressing cells. A likely explanation for these observations is that, in the absence of retromer function, progression of Wingless along the secretory pathway becomes blocked or impaired. Transverse reconstructions of imaginal discs show that Wingless is found throughout the apico-basal axis in *Vps35*-deficient tissue, while in the wild type, it accumulates in the apical half of the epithelium (Fig. 1i, j). We cannot distinguish at this point if apico-basal targeting, or a block in secretion, is the primary defect.

Previous findings in *C. elegans* suggested that lack of *Vps35* might preferentially affect long range signalling, while leaving short range signalling unaffected¹. To distinguish between short and long range Wingless signalling in *Drosophila* imaginal discs, we used two target genes: *senseless*, a high level target that is expressed in cells flanking the Wingless source³ and *distalless (dll)*, a medium/low level target¹⁸, which is expressed in most of the wing pouch. Expression of *senseless* is strongly reduced in *Vps35*-deficient posterior compartments (Fig. 2a, b). Therefore, contrary to expectation from the *C. elegans* results, expression of this juxtacrine target gene requires retromer function. No appreciable effect on *dll* expression was detected (Fig. 2c, d). One possibility is that residual Wingless found in the extracellular space of *Vps35*-deficient tissue is sufficient to activate this low level target. Significantly however, the loss of *senseless* expression is consistent with a reduction of Wingless secretion in *Vps35* mutant tissue and indicates an important role for *Vps35* in short range Wingless signalling.

Is *Vps35* generally needed for secretion or is it specifically involved in Wingless secretion? A general requirement for secretion is unlikely because knocking down *Vps35* in S2 cells by RNAi results in an increase, not a decrease, in the secretion of a generic secreted molecule (Luciferase carrying a minimal signal peptide; Wendler, unpublished observation). To assess specificity *in vivo*, we examined the behaviour of another signalling molecule, Hedgehog, in *Vps35* mutant tissue. Hedgehog is normally expressed in the posterior compartment and activates target genes such as *patched* along the compartment boundary¹⁹. Clones of *Vps35* mutant cells were induced at early larval stages with *heat shock-Flp (hs-Flp)* and resulting imaginal discs were simultaneously stained with anti-Wingless and anti-Hedgehog (with the standard protocol). Accumulation of Wingless is readily seen in *Vps35*-deficient *wingless*-expressing cells, as shown above in Fig. 1h. By contrast, Hedgehog does not accumulate in mutant tissue. To confirm that *Vps35* is not required for Hedgehog secretion,

we assessed the expression of *patched*, a target of Hedgehog signalling, under conditions where most of the Hedgehog-expressing tissue (the posterior compartment) is made *Vps35* mutant²⁰. As can be seen in Fig. 2h, *patched* expression appears to be normal (compare to Fig. 2i). We conclude that the retromer is required for a specific step in the secretion of Wingless while it appears dispensable for Hedgehog secretion. It is also dispensable for Notch secretion since, *wingless* transcription, which requires Notch signalling^{21, 22}, is unaffected in *Vps35*-deficient tissue (Supplementary Fig. 1). Nevertheless, we cannot exclude the possibility that the retromer complex could be involved in the secretion of other proteins. The 7-pass transmembrane protein encoded by *wntless (wls)*⁴, a gene also known as *Evenness interrupted (Evi)*⁵ or *sprinter*⁶, has recently been shown to be specifically required for Wingless secretion. The current model is that Wls binds Wingless in the Golgi apparatus, escorts it to the plasma membrane and releases it there⁴⁻⁶. In the absence of Wls, Wingless would be unable to leave the Golgi. One can envision that, after delivering Wingless to the plasma membrane, Wls might be internalised by endocytosis, recycled back to the Golgi by a retromer-dependent process and thus become available for another round of Wingless transport. Accordingly, in *Vps35*-deficient cells, Wls would no longer return to the Golgi and Wingless could only rely on newly synthesised Wls for transport to the plasma membrane. If this were indeed the case, boosting the production of Wls should restore Wingless secretion in *Vps35* mutant tissue. We tested this prediction by generating posterior compartments that, at the same time as being mutant for *Vps35*, overexpress Wls (see materials and methods). In this experimental setup, the anterior compartment remains wild type (*Vps35*⁺ and not overexpressing Wls). The level of Wingless in expressing cells is still slightly higher in the *Vps35* mutant compartment than in the wild type. However, punctate staining is clearly seen within responding cells of the mutant compartment, indicating that Wingless is secreted and spreads despite the absence of *Vps35* activity (Fig. 3a, b). This is also apparent in a fluorescence profile shown in the inset of Fig. 3 b. For comparison, little Wingless is detectable in *Vps35* mutant compartments that do not overexpress Wls (Fig. 1 h). We conclude that overexpressed Wls rescues the Wingless secretion phenotype of *Vps35* mutant cells. This is a strong indication that these two proteins operate in the same pathway.

In the above rescue experiment, most but not all posterior cells are *Vps35* mutant while all posterior cells uniformly overexpress V5-tagged Wls under the control of *hedgehog-Gal4*. Despite being expressed at a uniform level in the posterior compartment, exogenous Wls (detected with anti-V5) appears less abundant in posterior *Vps35* mutant cells than in nearby posterior wild type cells (Fig. 3c,d). Fluorescence intensity was measured in randomly chosen regions of interest (ROIs) within wild type and *Vps35* territories from 5 imaginal discs. *Vps35* mutant cells contained on average ~40% less fluorescence (16.30 ± 3.98 arbitrary intensity units; 10 ROIs) than control cells (27.09 ± 7.69 arbitrary intensity units; 10 ROIs), a statistically significant reduction (t test, one tailed, $p=0.0000306$). This observation suggests that the stability of Wls is reduced in the absence of *Vps35* activity. To further investigate this suggestion, we asked if the level of human Wls (hWls) is also affected by the loss of retromer activity. Human Wls was tagged with a Flag epitope and expressed in HEK293 cells. Cells were then treated with siRNA against human *Vps35* and cell extracts were probed by Western blots. Probing with anti-*Vps35* antibodies shows that the siRNA is effective (Lane 4, *Vps35* band in Fig. 3e). The amount of *Vps26*, another

component of the retromer (but not that of a control protein, β -tubulin) is also reduced. A likely explanation is that the complex must be intact for individual components to remain stable¹⁶. Importantly, knocking down Vps35 by siRNA leads to a mild but significant decrease in Wls level (densitometry analysis shows that intensity of the Wls band drops by 18% in siRNA treated cells relative to control cells; paired t test $p < 0.05$). This finding adds to the evidence that the stability of Wls decreases upon reduction of Vps35 activity. One possibility is that, in the absence of retromer function, internalised Wls is diverted to degradative compartments instead of being returned to the Golgi. We set out to investigate this prediction by immuno-electron microscopy (EM) in wing imaginal discs.

The *hedgehog-gal4* driver was used to express exogenous V5-tagged Wls in wing imaginal discs and, at the same time, to induce *Vps35* mutant clones in the posterior compartment. Larvae without *Vps35* mutant clones, but still expressing tagged Wls were used as a control. Experimental and control wing discs were treated for immuno-EM and ultrathin sections were labelled with anti-V5. In control discs, Wls was found mostly at the plasma membrane with a clear bias for the basolateral surface (Fig. 4 a and b). Wls was also seen, though to a lesser extent, in the ER, the Golgi and MVBs (Fig. 4 c-e). By contrast, as shown in (Fig. 4 f-h), a large number of gold particles can be seen in multivesicular bodies (MVBs) of *Vps35* mutant discs: 1.27 ± 0.98 gold particles per MVB square area ($n=17$) while 0.36 ± 0.27 gold particles per MVB square area ($n=20$) were seen in wild type control discs. Statistical analysis shows that the difference is highly significant (t test, one tailed; $p=0.000342$). We conclude that, in the absence of retromer function Wls is diverted to MVBs.

To test the possibility of a physical interaction between retromer components and Wls, we performed immunoprecipitation experiments with extracts from HEK293 cells. Flag-tagged hWls was expressed and cell extracts were immunoprecipitated with anti-Vps26 antibodies. Both Vps35 and Wls were detected in the immunoprecipitate (Fig. 4 i, j). The presence of Vps35 is consistent with the fact that it is part of the retromer complex with Vps26. The presence of hWls provides strong evidence that hWls forms a complex with retromer components, lending support to the idea that Wls is a specific retromer cargo.

So far all our data are consistent with the idea that the Golgi is continuously replenished with Wls by retromer-dependent retrograde transport. In the steady state, a significant amount of exogenously expressed hWls is present in the Golgi of HEK293 cells and this is strongly reduced following treatment with *Vps35* siRNA (supplementary figure 2). Therefore the retromer complex is required to maintain a steady supply of Wls in the Golgi. To directly assess retrograde transport, we introduced a 2xV5 tag on the N-terminal (extracellular domain) of hWls-Flag to generate 2xV5-hWls-Flag and expressed this protein in HEK293 cells. This construct allowed us to track the fate of internalised Wls following surface labelling. As can be seen in Fig. 5 b-d, a significant amount of surface-labelled Wls is present in the Golgi after a 24 min chase. When the same experiment is performed with cells treated with *Vps35* siRNA, only very little Wls is seen in the Golgi (Fig. 5 f, g). Interestingly, under this condition, Wls appears to accumulate in non-Golgi intracellular vesicles, possibly endosomes (compare Figures 5 b and 5 f). These results provide strong evidence that Wls undergoes retrograde transport to the Golgi in a retromer-dependent manner.

All existing data suggest the following model (Fig. 5 i). After initial entry into the Golgi, Wls would progress with Wingless to the plasma membrane. Following dissociation from Wingless, Wls would then be endocytosed and returned to the Golgi in a retromer-dependent fashion. By virtue of being loaded with Wingless during the Golgi-to-plasma membrane leg and 'empty' on the way back from the cell surface to the Golgi, Wls would operate like a conveyor belt, continuously lifting Wingless from the Golgi to the plasma membrane. In normal cells, a majority of endocytosed Wls is targeted to the Golgi with only a small proportion being directed to a lysosomal compartment. When retromer function is disrupted (Fig. 5 j), the return route to the Golgi is cut off, causing increased targeting to degradative compartments. This would explain the increased localisation of Wls in MVBs and its apparent destabilisation in *Vps35*-deficient cells. Because of the conservation of all the proteins involved, and their interactions, we expect our model to be generally applicable to vertebrate Wnts. One remaining question relates to the mechanism that allows Wls to off-load Wnts at the plasma membrane thus allowing it to perform their biological function.

Materials And Methods

Molecular Biology

The coding region of *wls* (GC6210-A) was amplified with primers that introduced a V5 tag at the C-terminus. The primers also contained an *Eco* RI and an *Xba* I site so that the product could be introduced into pUAST to generate pUAST-Wls-V5. Germline transformants (*UAS-Wls-V5*) were obtained by standard methods. Human Wls-Flag (hWls-Flag) was obtained by PCR amplification from human EST clones (6065683 and 5186852) introducing a Flag tag at the C-terminus. *Eco* RI and *Xba* I were also used for cloning into pCS2⁺. 2xV5-hWls-Flag was generated by insertion of a double stranded oligonucleotide encoding 2 copies of the V5 epitope and a glycine linker (ATCGGCGGCGGCGGCGGCGGCGGTAAGCCTATCCCTAACCCCTCTCCTCGGTCTCGATTCTACGGGTAAGCCTATCCCTAACCCCTCTCCTCGGTCTCGATTCTACGGGCGGCGGCGGCGGC) into the unique *Eco* RV site of pCS2⁺ hWls-Flag (at position +648 in the ORF).

Drosophila genetics

A null mutation in *Vps35* was generated by imprecise excision of a P-element inserted at the 5' end of GC5625 (P[EPgy2]CG5625EY¹⁴²⁰⁰, obtained from Bloomington). Lethality of the resulting disruptions were verified over a deficiency in the region (*Df(2R)Exel6078*, also obtained from the Bloomington stock center). A deletion of nearly 2kb, which removes the first three exons including the translation start site was selected for further analysis. We refer to this allele as *Vps35^{MH20}*. This allele was recombined with *FRTG13* and *FRT42D* (both from Bloomington) to allow the generation of mutant clones by Flp-mediated mitotic recombination. To make randomly located clones, recombination was induced with *hs-Flp*. Alternatively, clones were targeted to the posterior compartment with *hedgehog-Gal4* and *UAS-Flp*. Specifically, *w; FRT42D PCNA Ubi-GFP/+; hedgehog-Gal4 UAS-Flp/+* males were crossed to *w; FRT42D Vps35^{MH20}/CyO* females. For the rescue experiment, *w; FRT42D PCNA Ubi-GFP/+; hedgehog-Gal4 UAS-Flp/+* males were crossed to *w; FRT42D Vps35^{MH20}/GlaBc; UAS-Wls-V5/+* females. Germline clones were induced with

yw; *FRTG13 ovo^D* and *hs-Flp*. The stocks needed for these crosses were all obtained from Bloomington except for *hedgehog-Gal4* (A gift from Jose Casal, University of Cambridge), which was recombined with *UAS-Flp* for this study. *UAS-Wls-V5* transformants were also generated for this study (see Molecular Biology).

Antibodies

Primary antibodies used for immunofluorescence were: mouse anti-Wingless 4D4 (prepared from cells obtained from the Developmental Studies Hybridoma Bank), mouse anti-V5 (Invitrogen; 1/1000), rabbit anti-Hedgehog (from Suzanne Eaton, MPI Dresden), mouse anti-Patched (from Isabel Guerrero, Universita Autonoma Madrid), rabbit anti-GFP (Abcam; 1/2500), mouse anti-Distal-less (from Ian Duncan, University of Wisconsin; 1/500) guinea pig anti-Senseless (from Hugo Bellen, Baylor College of Medicine; 1/1000), and sheep anti-TGN46 (Serotec; 1/100). Secondary antibodies for immunofluorescence were from Molecular Probes: Alexa488-conjugated goat anti-rabbit (1/200), Alexa488-conjugated goat anti-mouse (1/200), Alexa555-conjugated goat anti-mouse (1/200), Alexa594-conjugated goat anti-guinea pig (1/200), and Alexa488-conjugated donkey anti-sheep (1/200). For Western blots, the following primary antibodies were used: HRP-conjugated anti-Flag (M2, Sigma; 1/5000), rabbit anti-Vps35 and rabbit anti-Vps26 (both from Matthew Seaman, University of Cambridge; 1/100), mouse anti- β -tubulin (T4026, Sigma, 1/2000), and mouse anti-GFP (Roche, clones 7.1 and 13.11; 1/2000). Western blots were developed using Pierce ECL Western Blotting Substrate (34096).

Immuno electron microscopy

Larvae were inverted in Ringer solution, fixed in 2% PFA and 0.2% glutaraldehyde in 0.1 M phosphate buffer (PB) pH7.4 for 3 hours at room temperature, washed in PBS and kept in 1% PFA/PBS at 4°C. Wing discs were dissected, embedded in 12% gelatin, mounted on aluminium pins and frozen in liquid nitrogen. Frozen wing discs were sectioned on a Reichert Ultracut S cryotome at -120°C. Antibody- and gold-labelling procedures were performed as described previously²³. Sixty-nanometer-thick cryosections were incubated with anti-V5 antibodies, rabbit anti-mouse IgG (DakoCytomation Denmark A/S, Glostrup, Denmark) followed by protein A conjugated to 10- or 15-nm gold particles.

Immunoprecipitation

For immunoprecipitation experiments, cells were plated on 100 mm plates and transfected with PolyFect (Qiagen) following the manufacturer's protocol. Cells were then incubated for 48 hours prior to collection. All subsequent steps were performed at 4°C. Cells were washed in PBS and incubated for 20 minutes with 1 ml of extraction buffer (50 mM Tris pH 7.5, 150 mM NaCl, 1mM EDTA, 1% Triton X-100) containing a complete protease inhibitor mix (Roche). The cell lysate was centrifuged for 10 minutes at 12000 rcf and the supernatant was collected. The lysate was pre-incubated with protein A sepharose beads (GE Healthcare) for 1 hour. After the removal of the beads, the lysate was incubated with anti-Vps26 (1:150) for 2 hours, followed by further incubation with fresh protein A beads for overnight. Washing was performed 4 times in TBS (50 mM Tris pH 7.5, 150 mM NaCl). Dried protein A beads were boiled for 5 minutes with 30 μ l of Laemmli sample buffer (Bio-Rad) in the absence of

reducing agents. The supernatant was then collected and further incubated for 1 hour at 37°C with reducing agents prior to Western Blotting.

siRNA

Lipofectamine 2000 (Invitrogen) was used to co-transfect siRNA and DNA in HEK293 cells, following the manufacturer's protocol. For 35 mm plates, we used 5 µl of Lipofectamine 2000, 750 ng of total DNA and 50 pmol of siRNA. Three different siRNA were tested for the silencing of *Vps35*. Of these, only 2 proved effective as assayed by immunocytochemistry (Ambion siRNA IaD # 132355 and 132357). Both were used as a 1:1 mixture in subsequent experiments. Ambion's negative control #1 was used as a control siRNA. Cell extracts were prepared as for immunoprecipitation experiments except that smaller volumes were used (150 µl of extraction buffer for a 35 mm plate).

Antibody uptake

Antibody uptake was performed with HEK293T cells transfected with V5-hWls-Flag grown on coverslips. Cells were labelled with a 2.24mg/ml solution of anti-V5 in culture medium and subsequently treated as described by Seaman¹⁶ (see also the legend of Fig. 5).

Supplementary Material

Refer to Web version on PubMed Central for supplementary material.

Acknowledgements

We thank M. Seaman, S. Eaton, H. Bellen, I. Duncan, I. Guerrero, and the Developmental Studies Hybridoma Bank (Iowa University) for antibodies. We also thank the Bloomington Stock Center (Indiana University) for numerous *Drosophila* strains. This work was largely funded by the Medical Research Council of Great Britain. Additional funding was provided by the Endotrack program of the European Union (to FW and JPV) and the Dutch Cancer Society grant UU2006-3508 (to MM). Cyrille Alexandre, Matthew Hannah and Iris Salecker provided critical comments to the manuscript.

References

1. Coudreuse DY, Roel G, Betist MC, Destree O, Korswagen HC. Wnt gradient formation requires retromer function in Wnt-producing cells. *Science*. 2006; 312 :921–924. [PubMed: 16645052]
2. Prasad BC, Clark SG. Wnt signaling establishes anteroposterior neuronal polarity and requires retromer in *C. elegans*. *Development (Cambridge, England)*. 2006; 133 :1757–1766.
3. Nolo R, Abbott LA, Bellen HJ. Senseless, a Zn finger transcription factor, is necessary and sufficient for sensory organ development in *Drosophila*. *Cell*. 2000; 102 :349–362. [PubMed: 10975525]
4. Banziger C, et al. Wntless, a conserved membrane protein dedicated to the secretion of Wnt proteins from signaling cells. *Cell*. 2006; 125 :509–522. [PubMed: 16678095]
5. Bartscherer K, Pelte N, Ingelfinger D, Boutros M. Secretion of Wnt ligands requires Evi, a conserved transmembrane protein. *Cell*. 2006; 125 :523–533. [PubMed: 16678096]
6. Goodman RM, et al. Sprinter: a novel transmembrane protein required for Wg secretion and signaling. *Development (Cambridge, England)*. 2006; 133 :4901–4911.
7. Strigini M, Cohen SM. Wingless gradient formation in the *Drosophila* wing. *Curr Biol*. 2000; 10 :293–300. [PubMed: 10744972]
8. Struhl G, Basler K. Organizing activity of wingless protein in *Drosophila*. *Cell*. 1993; 72 :527–540. [PubMed: 8440019]

9. Vincent JP, Dubois L. Morphogen transport along epithelia, an integrated trafficking problem. *Dev Cell*. 2002; 3 :615–623. [PubMed: 12431369]
10. Zhu AJ, Scott MP. Incredible journey: how do developmental signals travel through tissue? *Genes Dev*. 2004; 18 :2985–2997. [PubMed: 15601817]
11. Takada R, et al. Monounsaturated fatty acid modification of Wnt protein: its role in Wnt secretion. *Dev Cell*. 2006; 11 :791–801. [PubMed: 17141155]
12. Willert K, et al. Wnt proteins are lipid-modified and can act as stem cell growth factors. *Nature*. 2003; 423 :448–452. [PubMed: 12717451]
13. Panakova D, Sprong H, Marois E, Thiele C, Eaton S. Lipoprotein particles are required for Hedgehog and Wingless signalling. *Nature*. 2005; 435 :58–65. [PubMed: 15875013]
14. Mikels AJ, Nusse R. Wnts as ligands: processing, secretion and reception. *Oncogene*. 2006; 25 :7461–7468. [PubMed: 17143290]
15. Hausmann G, Banziger C, Basler K. Helping Wingless take flight: how WNT proteins are secreted. *Nat Rev Mol Cell Biol*. 2007; 8 :331–336. [PubMed: 17342185]
16. Seaman MN. Cargo-selective endosomal sorting for retrieval to the Golgi requires retromer. *J Cell Biol*. 2004; 165 :111–122. [PubMed: 15078902]
17. Seaman MN. Recycle your receptors with retromer. *Trends Cell Biol*. 2005; 15 :68–75. [PubMed: 15695093]
18. Jaiswal M, Agrawal N, Sinha P. Fat and Wingless signaling oppositely regulate epithelial cell-cell adhesion and distal wing development in *Drosophila*. *Development (Cambridge, England)*. 2006; 133 :925–935.
19. Hidalgo A, Ingham P. Cell patterning in the *Drosophila* segment: spatial regulation of the segment polarity gene patched. *Development (Cambridge, England)*. 1990; 110 :291–301.
20. Tabata T, Kornberg TB. Hedgehog is a signaling protein with a key role in patterning *Drosophila* imaginal discs. *Cell*. 1994; 76 :89–102. [PubMed: 8287482]
21. Rulifson EJ, Blair SS. Notch regulates wingless expression and is not required for reception of the paracrine wingless signal during wing margin neurogenesis in *Drosophila*. *Development (Cambridge, England)*. 1995; 121 :2813–2824.
22. Diaz-Benjumea FJ, Cohen SM. Serrate signals through Notch to establish a Wingless-dependent organizer at the dorsal/ventral compartment boundary of the *Drosophila* wing. *Development (Cambridge, England)*. 1995; 121 :4215–4225.
23. Liou W, Geuze HJ, Slot JW. Improving structural integrity of cryosections for immunogold labeling. *Histochem Cell Biol*. 1996; 106 :41–58. [PubMed: 8858366]

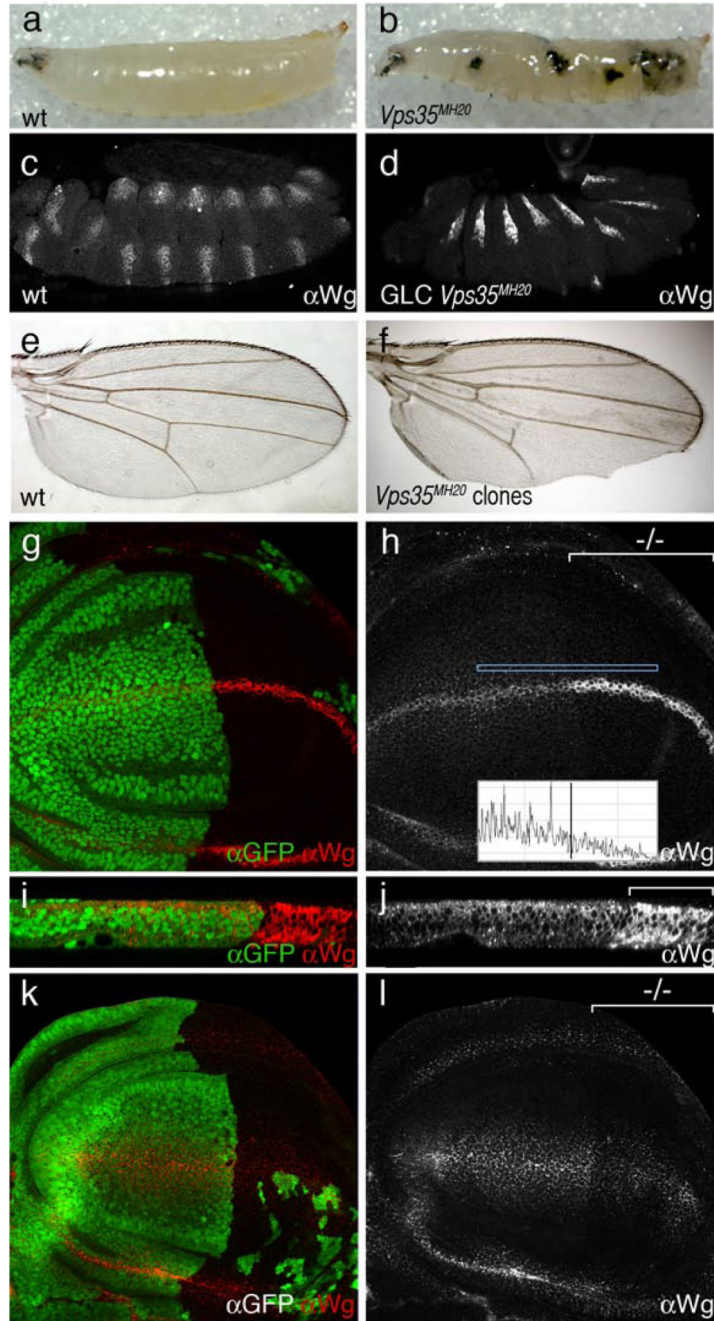


Figure 1. Reduced Wingless secretion in *Vps35* mutant cells.

(a) Wild type larva at the 3rd instar stage. (b) Melanotic tumours in a homozygous *Vps35*^{MH20} larva of the same stage. The same phenotype is seen in *Vps35*^{MH20}/*Df(2R)Exel6078* larvae. (c) Expression of Wingless in a wild type stage 14 embryo as detected with an anti-Wingless antibody. (d) Embryo of a similar stage lacking maternal and zygotic *Vps35* (obtained from germ line clones). Increased level of Wingless protein within *wingless*-expressing cells can be seen. Note here that Engrailed expression is still detected in these embryos (not shown) suggesting that some Wingless activity is present.

(e) Wild-type adult wing. (f) Adult wing carrying unmarked *Vps35^{MH20}* homozygous clones. Note the notched margin, an indication of deficient Wingless signalling. (g, h) Conventional anti-Wingless staining of imaginal discs harboring *Vps35* mutant cells in most of the posterior compartment (-/- marks the mutant compartment). The anterior compartment (GFP-positive) is wild type. Note the relative accumulation of Wingless (red in g, white in h) in *Vps35* deficient, *wingless*-expressing cells. Note also the reduced punctate staining in non-expressing cells. This was quantified by plotting the fluorescence intensity along the antero-posterior within the rectangle shown (inset in h). (i, j) Transverse reconstruction of the Wingless-expressing domain from the samples shown in panels g and h. Accumulation of Wingless in the posterior cells is readily seen. Accumulation appears to be throughout the apico-basal axis. (k, l) Extracellular Wingless in an imaginal disc with a posterior compartment that is mostly *Vps35* mutant (GFP-negative, marked by -/- in l). Staining is reduced in the mutant territory.

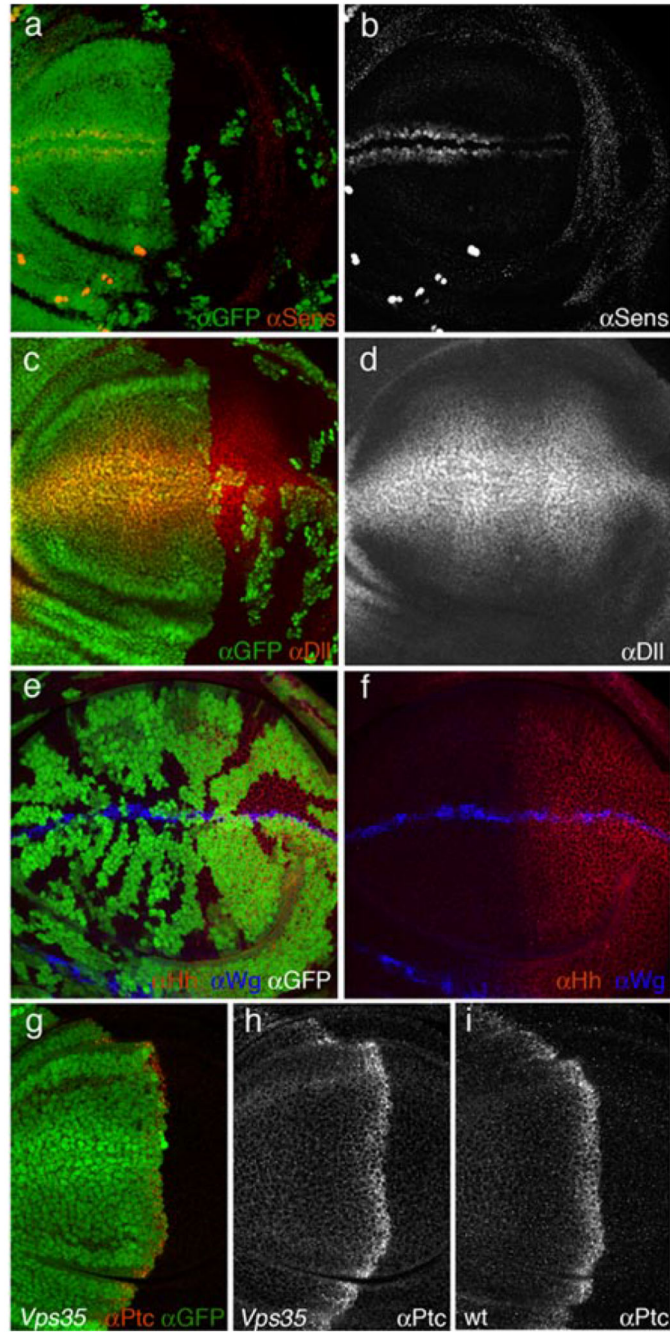
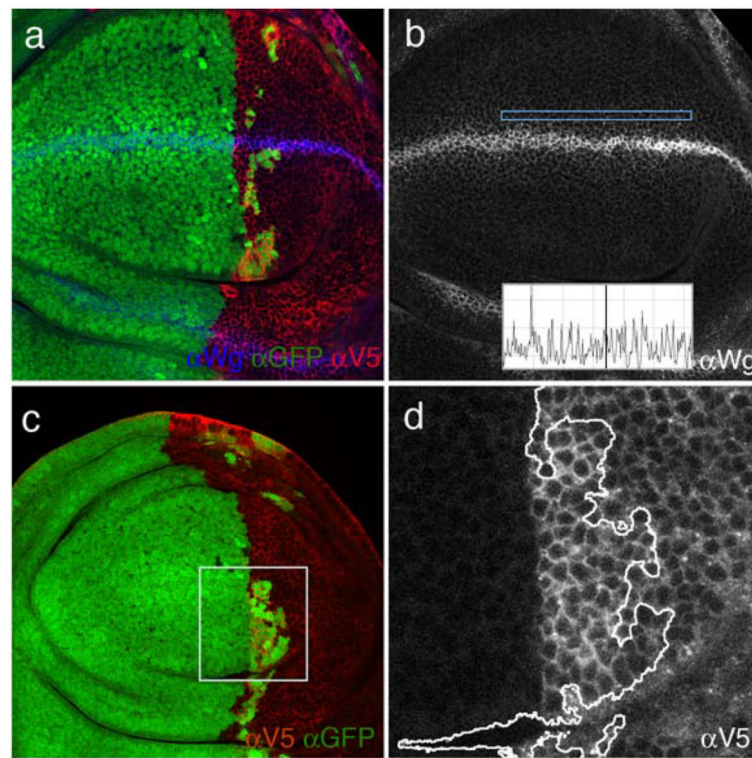


Figure 2. Wingless signalling but not Hedgehog signalling is impaired in *Vps35* mutant tissue. (a, b) Expression of *senseless* (red in a, white in b) in an imaginal disc with a posterior compartment that is mostly *Vps35* mutant. Expression is strongly reduced in the mutant (GFP-negative) tissue. (c, d) Expression of *Dll* (red in c, white in d) in an imaginal disc with a posterior compartment that is mostly *Vps35* mutant. No noticeable reduction of expression can be seen. (e, f) Expression of Hedgehog (red) in an imaginal disc harboring *Vps35* mutant clones (marked by the absence of GFP). A slight reduction is noticeable in the clones located within the Hedgehog expression territory. This is in stark contrast with the increased

Wingless staining (blue) in mutant Wingless-expressing cells. (g, h) Expression of Patched (red in g, white in h) in an imaginal disc with a posterior compartment that is mostly *Vps35* mutant. Expression is as in wild type discs. (i) Expression of Patched in a wild type imaginal disc.



e

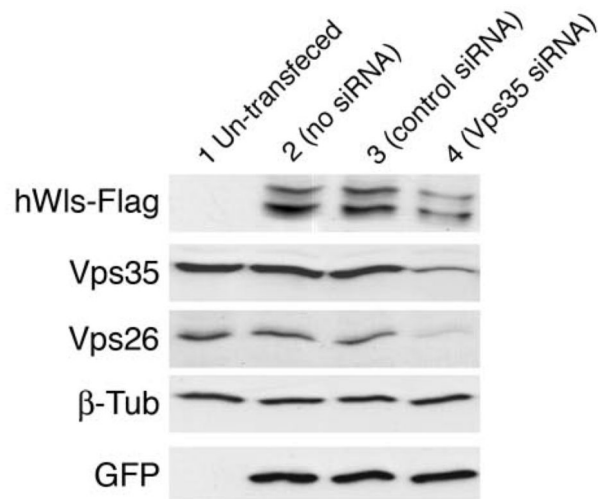


Figure 3. Rescue of Wingless secretion in *Vps35* mutant cells by overexpressed Wls and reduced stability of Wls in the absence of *Vps35* activity.

(a-b) All the cells of the posterior compartment express Wls (Anti-V5 in red) and nearly all the posterior cells are mutant for *Vps35* (GFP-negative). Secretion of Wingless (blue in a, white in b) is rescued in the posterior compartment: punctate staining can be seen in non-expressing posterior cells. Rescue can also be seen in the fluorescence intensity profile (inset in b) (c, d) Same genotype as in a, b, but the Wingless channel is not shown. Wls-V5 is shown in white in d. Boxed area is selected because it contains both *Vps35*⁺ (GFP-positive) and *Vps35* mutant cells thus allowing a direct comparison at high

magnification. (d) Close-up of the boxed area in c. Anti-V5 staining shows that there is a lower level of Wls in *Vps35* mutant cells (right hand side of the wiggly line) than in *Vps35*⁺ cells. (e) Western blot of extracts from HEK293 cells. Extracts were probed with various antibodies as indicated on the left. Cells were transfected as follows for each lane: empty vector alone (lane 1), *GFP* + *hWls-Flag* (lane 2), *GFP* + *hWls-Flag* + control siRNA (lane 3), and *GFP* + *hWls-Flag* + *Vps35* siRNA (lane 4). Note the reduction in Vps35, Vps26, and Wls in lane 4. Note also that two bands of Wls are detected, suggesting that this protein may undergo post-translational processing.

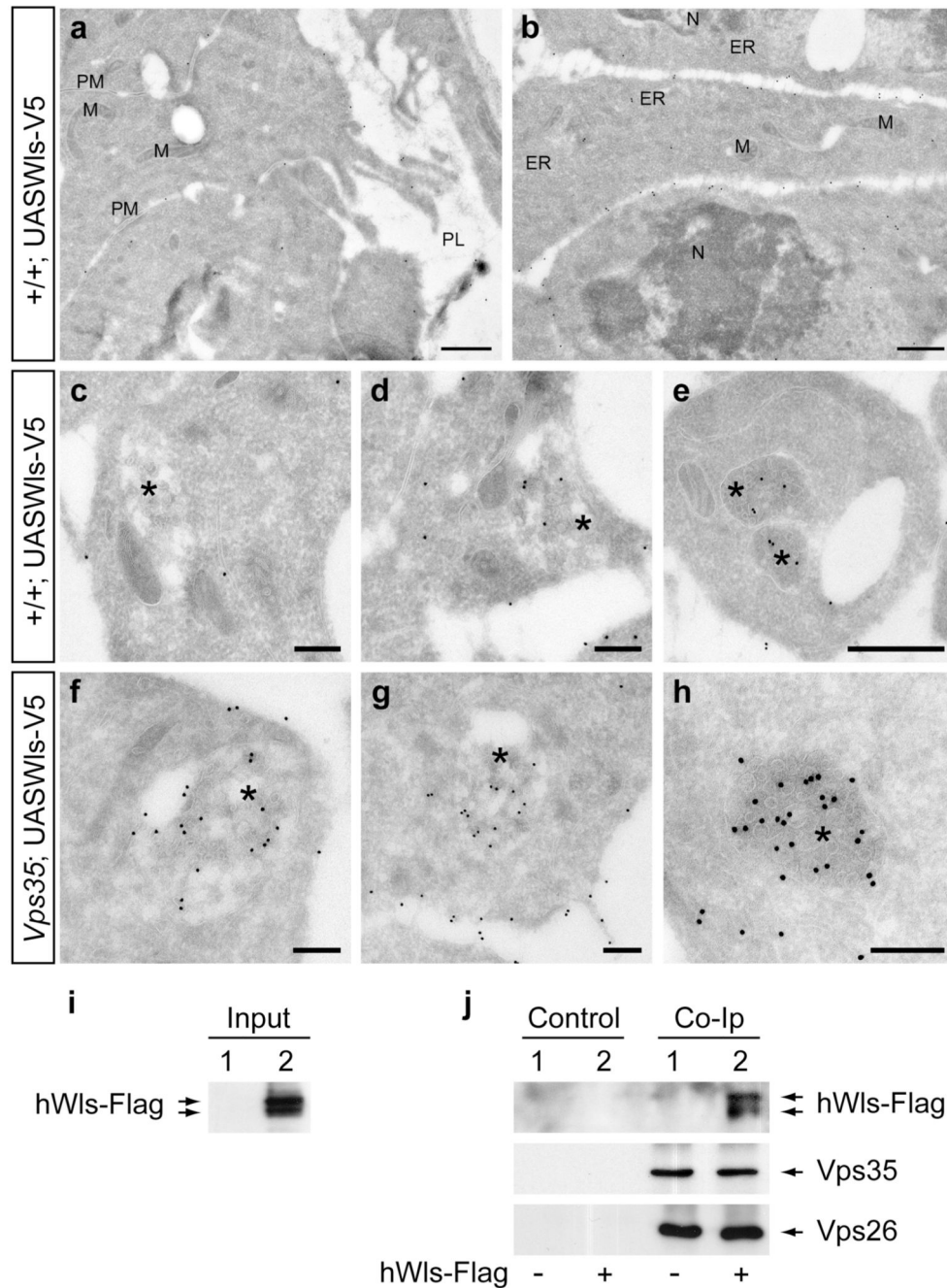


Figure 4. Accumulation of Wls in MVBs of retromer-deficient cells and physical interaction between Wls and retromer components.

(a) Apical region of wild-type wing disc cells in the posterior compartment overexpressing Wls-V5. Wls is visualized with anti-V5 and secondary antibody labelled with 15 nm gold particles. Empty space represents the peripodial lumen (PL). Relatively few gold particles can be seen at the apical membranes. (b) By contrast, abundant signal is detected in the basolateral region of Wls-V5 expressing cells. (c-e) Moderate labelling of MVBs in wild type cells expressing Wls-V5. Examples are representative of 20 MVBs analyzed. (f-h) Wls strongly accumulates in MVBs in retromer mutant wing disc cells. Examples are

representative of 18 MVBs analyzed. M, Mitochondrion, N, Nucleus, PL, peripodial lumen, PM, plasma membrane. (i) Western blot of extracts from HEK293 cells transfected with empty plasmid (lane 1) or cells transfected with a hWls-Flag-expressing plasmid (lane 2). The blot was probed with anti-Flag and, as expected, signal is only seen in lane 2. These extracts were used as input for immunoprecipitation. (j) Western blot of immunoprecipitated material either in the absence (Control) or presence (Co-IP) or anti-Vps26 antibody. Input came either from mock-transfected cells (1) or from cells expressing hWls-Flag (2) as indicated with - or + at the bottom. The blot was first probed anti-Flag to detect hWls-Flag (top row) and subsequently re-probed to detect Vps35 and Vps26 (middle and lower panel). hWls-Flag is only detected from extract of hWls-transfected immunoprecipitated with anti-Vps26 antibody.

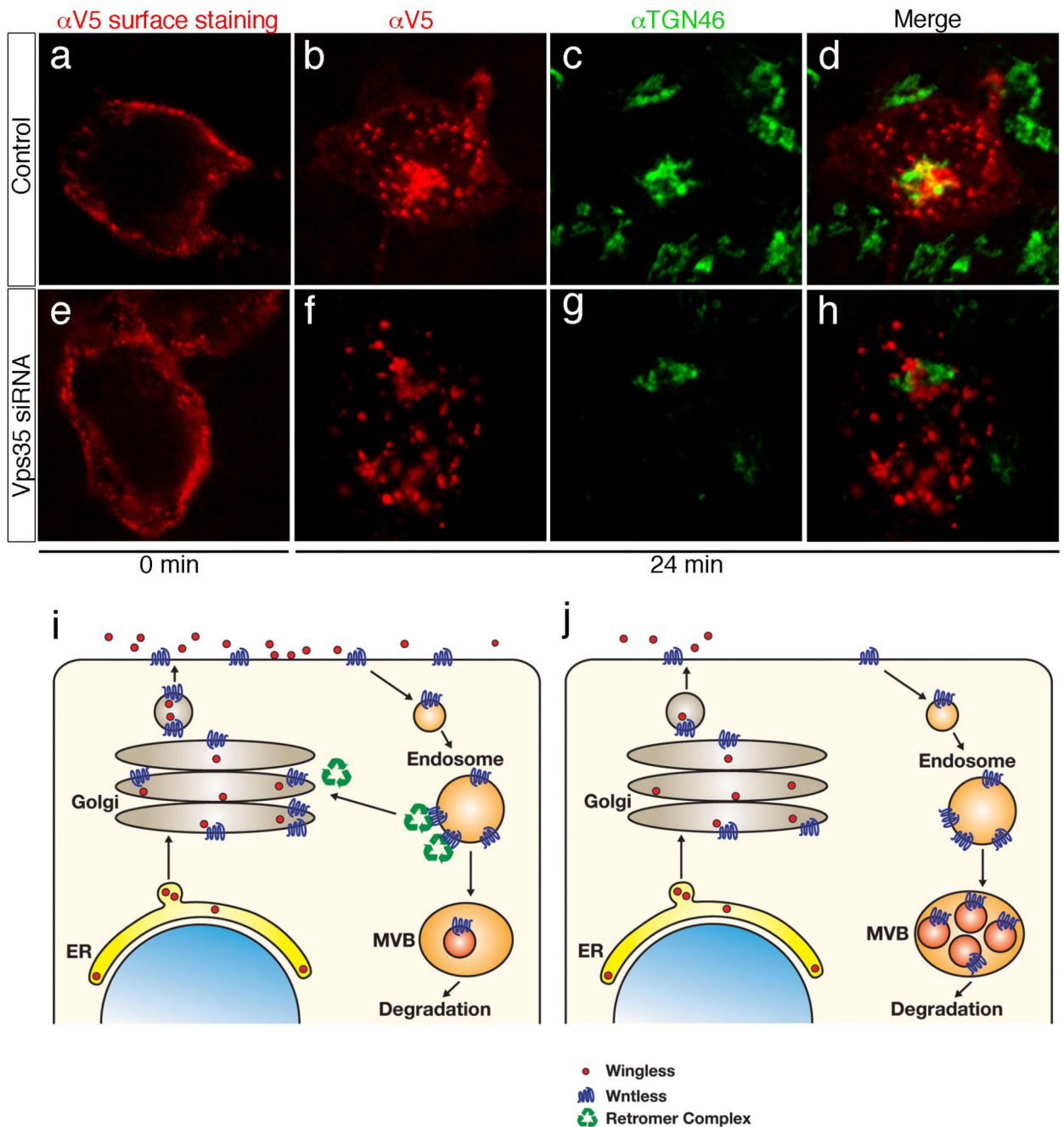


Figure 5. Retrograde transport of Wls and a model of how this ensures efficient Wingless secretion.

(a-d) HEK293T cells expressing 2xV5-hWls-Flag were incubated with anti-V5 antibodies for 30 minutes at 0°C, washed, and then either fixed (0 min; panel a) or incubated at 37 °C for 24 min (panels b-d). Cells were then fixed, permeabilized and stained with anti-TGN46 (green) to reveal internalized anti-V5 antibodies (red). Note the presence of anti-V5 (hWls) in TGN46-positive structures. (e-h) Same experiment as in panels a-d except that cells were co-transfected with siRNA against *Vps35*. Staining with anti-V5 at 0 min shows that *Vps35* knock down does not significantly affect Wls secretion. Following the 24 min chase, no

significant co-localization is seen between anti-V5 and TGN46-positive structures (compare panel h with panel d). (i) Model of the role of Wls in Wingless secretion in wild type cells. We suggest that Wingless binds Wls in the Golgi. From there, the two proteins travel together to the plasma membrane where they dissociate, allowing Wingless to signal or to be transported towards distant target cells. Following dissociation from Wingless, empty Wls is internalised by endocytosis. The retromer complex then retrieves Wls from endosomes and directs it back to the Golgi thus making it available for another round of transport. (b) In the absence of retromer activity, newly synthesised Wls can reach the plasma membrane and be endocytosed. However, as the retromer-dependent route to the Golgi is no longer accessible, endocytosed Wls progresses to multi-vesicular-bodies (MVBs) and lysosomes and is degraded.